On the Energy Efficiency of THz-NOMA enhanced UAV Cooperative Network with SWIPT

Jalal Jalali *Member, IEEE*, Ata Khalili *Member, IEEE*, Hina Tabassum *Senior Member, IEEE*, Rafael Berkvens *Member, IEEE*, Jeroen Famaey *Senior Member, IEEE*, and Walid Saad *Fellow, IEEE*.

***Abstract*—This paper considers the energy efficiency (EE) maximization of a simultaneous wireless information and power transfer (SWIPT)-assisted unmanned aerial vehicles (UAV) cooperative network operating at TeraHertz (THz) frequencies. The source performs SWIPT enabling the UAV to receive both power and information while also transmitting the information to a designated destination node. Subsequently, the UAV utilizes the harvested energy to relay the data to the intended destination node effectively. Specifically, we maximize EE by optimizing the non-orthogonal multiple access (NOMA) power allocation coefficients, SWIPT power splitting (PS) ratio, and UAV trajectory. The main problem is broken down into a two-stage optimization problem and solved using an alternating optimization approach. In the first stage, optimization of the PS ratio and trajectory is performed by employing successive convex approximation using a lower bound on the exponential factor in the THz channel model. In the second phase, the NOMA power coefficients are optimized using a quadratic transform approach. Numerical results demonstrate the effectiveness of our proposed resource allocation algorithm compared to the baselines where there is no trajectory optimization or no NOMA power or PS optimization.**

***Index Terms*—Cooperative Communication, Energy Efficiency, NOMA, SWIPT, THz, UAV.**

I. Introduction

THE use of unmanned aerial vehicles (UAVs) in radio access networks has drawn significant attention in the past few years as it offers many benefits, such as wide coverage, mobility, and line-of-sight (LoS) connectivity [1]. Since commercial UAVs have limited energy resources with significant energy consumption, energy efficient design is always critical for UAV-assisted networks. In this context, simultaneous wireless information and power transfer (SWIPT) [2] is a technique which enables extending the UAV's battery lifespan – improving the network's energy efficiency (EE) [3].

To date, a variety of research works considered throughput, coverage, or reliability maximization in SWIPT-assisted UAV networks. In [4], SWIPT-assisted UAV is considered, and the harvested power at the UAV is applied to retransmit information to the destination node. In particular, network throughput maximization was performed by considering a cooperative link between source and destination. In [5], UAV-assisted cooperative communication was studied where throughput was maximized under UAV's mobility and harvested power. Also, in [6], the performance of downlink UAV-assisted SWIPT was analyzed in terms of security, reliability, and coverage.

Nevertheless, since the next-generation wireless networks will need to support massive connectivity and extreme data rates [7], it is becoming crucial to integrate advanced wireless technologies into UAV networks. Thus, combining the benefits of extreme bandwidths offered by TeraHertz (THz) spectrum at the PHYsical (PHY) layer and massive connectivity offered by non-orthogonal multiple access (NOMA) at the Medium ACcess (MAC) layer would be of immediate relevance [8].

Recently, a few research studies considered THz-enabled UAV communications [9]–[11]. In [9], the authors considered a UAV-assisted THz network to minimize latency while optimizing the UAV deployment, power assignment, and bandwidth allocation. The work in [10] developed a cooperative recharging-transmission strategy for powered UAV-aided THz downlink networks. Finally, the authors in [11] investigated the potential benefits of integrating NOMA-based UAVs into THz-based networks. The intricacy of the THz channel propagation modeling necessitates a novel framework for UAV deployment and network resource allocation policy design.

None of the aforementioned research works considered maximizing the EE of THz-NOMA enabled UAV cooperative network neither with SWIPT nor without SWIPT.

In this paper, we maximize the EE of a THz-NOMA-enabled UAV cooperative network where the UAV is supported through SWIPT. The source node transmits a superposed message signal that contains data for both the UAV and the destination node, with different power allocation coefficients. The signal received at the UAV is then split into two components using a power splitting (PS) SWIPT mechanism. One portion of the signal is dedicated to energy harvesting (EH), while the other is used for information decoding (ID). We optimize the PS ratio, UAV trajectory, and NOMA power allocation coefficients by deriving a lower bound on the exponential term in the THz channel model and applying successive convex approximation and quadratic transform methods. Numerical results yield up to 30.3% performance gain compared to the case with no trajectory optimization.

II. System Model and Problem Formulation

We study a downlink transmission UAV-aided SWIPT-NOMA cooperative system. As shown in Fig. 1, the source node transmits information to two nodes, i.e., a UAV and a destination node. The UAV can act as an EH aerial relay to ensure the high targeted rate of the destination node. A three-dimensional (3D) Cartesian coordinate system are considered where the source and destination nodes are placed at $\boldsymbol{s}(t) = [s_x(t), s_y(t), H]^{\mathrm{T}} \in \mathbb{R}^{3\times 1}$ and $\boldsymbol{d}(t) = [d_x(t), d_y(t), 0]^{\mathrm{T}} \in \mathbb{R}^{3\times 1}$, respectively, where $[\cdot]^{\mathrm{T}}$ is the transpose operation. The destination node is static on the ground, while the UAV and source are at a fixed height above the ground. The instantaneous coordinates of the UAV are given by $\boldsymbol{q}(t) = [x(t), y(t), H]^{\mathrm{T}} \in \mathbb{R}^{3\times 1}$ at time $0 < t < T$. The first and final positions of the UAV are represented by $\boldsymbol{q}_s$ and $\boldsymbol{q}_e$, respectively. We assume that the UAV's trajectory regularly

varies over time, so the time range T is divided into N evenly separated time slots, where $\boldsymbol{q}[n], \forall n \in \mathcal{N}$ is the sampled trajectory. The constraints related to the position of the UAV and its maximum speed can be written as:

$$\boldsymbol{q}[1] = \boldsymbol{q}_s, \tag{1a}$$

$$\boldsymbol{q}[N+1] = \boldsymbol{q}_e, \tag{1b}$$

$$\|\boldsymbol{q}[n+1] - \boldsymbol{q}[n]\| \leq V_{\max}\delta, \ \forall n, \tag{1c}$$

where $V_{\max}$ is the maximum flying velocity of the UAV. The channel power gain between source-to-UAV and UAV-to-destination are denoted by $h_{sr}[n]$ and $h_{rd}[n]$, respectively. The channels are assumed to follow the free-space path loss model and are given by:

$$h_{sr}[n] = \frac{\beta_0}{\|\boldsymbol{q}[n] - \boldsymbol{s}[n]\|} e^{-\frac{\xi(f)}{2}\|\boldsymbol{q}[n]-\boldsymbol{s}[n]\|}, \forall n, \tag{2}$$

$$h_{rd}[n] = \frac{\beta_0}{\|\boldsymbol{q}[n] - \boldsymbol{d}[n]\|} e^{-\frac{\xi(f)}{2}\|\boldsymbol{q}[n]-\boldsymbol{d}[n]\|}, \forall n, \tag{3}$$

where $\xi(f)$ is a molecular absorption coefficient that is influenced by the operating frequency f and the concentration of water vapor molecules. To simplify the notation, we will henceforth denote $\xi(f)$ as ξ. Moreover, β_0 denotes the reference power gain and is equal to $c/4\pi f$, where c is the speed of light [10]. Finally, the channel power gain between the source-to-destination follows the same structure, as in (2) and (3), and is denoted by $h_{sd}[n]$.

The cooperative communication is executed in two phases. In the first phase, the UAV harvests energy and decode information from the source node while the destination node receives its respective data. In the second phase, the UAV acts as a decode-and-forward (DF) aerial relay to re-transmit the destination node's data using the harvested power of the first phase.

A. Phase One$^{(1)}$: Direct Transmission

In this phase, the source transmits the information to both the UAV and destination node by exploiting power-domain NOMA. Hence, the transmit signal is given by:

$$s[n] = \sqrt{\alpha_1[n]}s_1[n] + \sqrt{\alpha_2[n]}s_2[n], \forall n, \tag{4}$$

where $s_1[n]$ and $s_2[n]$ are transmit symbols during each time slot and assumed to be independently circularly symmetric complex Gaussian (CSCG) distributed with zero mean and unit variance. Moreover, $\sqrt{\alpha_1[n]}$ and $\sqrt{\alpha_2[n]}$ represent the NOMA power allocation coefficients in the n-th time slot, which need to satisfy the two following constraints:

$$\alpha_1[n] + \alpha_2[n] \leq P_{\text{peak}}, \forall n, \tag{5a}$$

$$\frac{1}{N}\sum_{n=1}^{N} \alpha_1[n] + \alpha_2[n] \leq P_{\max}. \tag{5b}$$

The received signal at the UAV can be expressed as:

$$y_r^{(1)}[n] = h_{sr}[n]s[n] + z_1^{(1)}[n], \forall n, \tag{6}$$

where $z_1^{(1)}[n] \sim \mathcal{N}(0, \sigma_1^2)$ is the received CSCG noise at the UAV node. By adopting a PS-SWIPT architecture, the received signal for ID and EH from the radio frequency (RF) source can be expressed as:

$$y_{\text{EH}}^{(1)}[n] = \sqrt{\rho[n]}\big(y_r^{(1)}[n]\big), \forall n, \tag{7}$$

$$y_{\text{ID}}^{(1)}[n] = \sqrt{1-\rho[n]}\big(y_r^{(1)}[n]\big) + z_2^{(1)}[n], \forall n, \tag{8}$$

where $0 < \rho[n] < 1$ is the PS ratio, and $z_2^{(1)}[n] \sim \mathcal{N}(0, \sigma_2^2)$ is the additional noise caused by the ID receiver. The UAV node employs a successive interference cancellation (SIC) receiver to decode the signals. In fact, the UAV first decodes the data of the destination node and then removes it from its received signal to obtain its own data in a successive manner. The received signal-to-interference-plus-noise-ratio (SINR) at the UAV to detect $s_2[n]$ can be stated as:

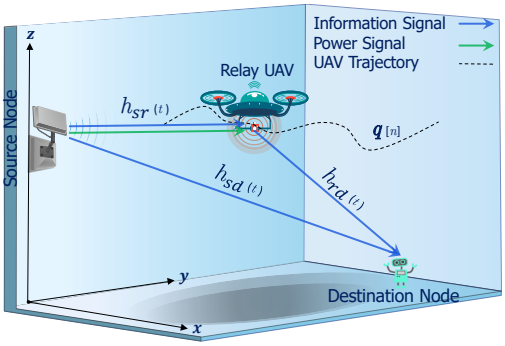

Fig. 1. UAV-assisted cooperative THz NOMA-SWIPT network.

$$\gamma_{d\leftarrow r}^{(1)}[n] = \frac{(1-\rho[n])\alpha_2[n]|h_{sr}[n]|^2}{(1-\rho[n])\alpha_1[n]|h_{sr}[n]|^2 + N}, \forall n, \tag{9}$$

where $N = (1-\rho[n])\sigma_1^2[n] + \sigma_2^2[n]$ is the equivalent total noise. Then, the corresponding SINR to decode UAV's data can be described as:

$$\gamma_r^{(1)}[n] = \frac{(1-\rho[n])\alpha_1[n]|h_{sr}[n]|^2}{N}, \forall n. \tag{10}$$

According to (6) and (7), the RF harvested power at the UAV by ignoring the noise power can be expressed as:

$$E[n] = \eta\rho[n]|h_{sr}[n]|^2\tau[n], \forall n, \tag{11}$$

where $\eta \in (0, 1]$ is the energy conversion efficiency and $\tau[n]$ is the transmission time fraction for the first phase during the n-th time slot. Besides, it is assumed that the transmission duration is the same for two phases, i.e., $\tau[n] = \frac{1}{2}$. Consequently, the transmit power at the UAV can be described by [5]:

$$P_t[n] = \frac{E[n]}{1-\tau[n]}, \forall n. \tag{12}$$

The received signal at the destination can be stated as:

$$y_d^{(1)}[n] = h_{sd}[n]s[n] + \nu_1{}^{(1)}[n], \forall n, \tag{13}$$

where $\nu_1{}^{(1)}[n] \sim \mathcal{N}(0, \delta_1[n])$ is the received noise at the destination node in the first phase. The SINR at the destination node to decode its own data can be written as:

$$\gamma_d^{(1)}[n] = \frac{\alpha_2[n]\ |h_{sd}[n]|^2}{\alpha_1[n]\ |h_{sd}[n]|^2 + \delta_1^2[n]}, \forall n. \tag{14}$$

B. Phase Two$^{(2)}$: Cooperative Transmission

In this phase, the UAV utilizes the harvested power to re-transmit the data of the destination node. Hence, the received signal at the destination node can be expressed as:

$$y_d^{(2)}[n] = \sqrt{P_t[n]}h_{rd}[n]s_2[n] + \nu_2{}^{(2)}[n], \forall n, \tag{15}$$

where $\nu_2{}^{(2)}[n] \sim \mathcal{N}(0, \delta_2^2[n])$ is the received noise at the destination node. The corresponding SINR reads as:

$$\gamma_d^{(2)}[n] = \frac{\eta\rho[n]|h_{sr}[n]|^2|h_{rd}[n]|^2}{\delta_2^2[n]}, \forall n. \tag{16}$$

Ultimately, the destination node uses the maximal ratio combination (MRC) to integrate the transmit signals from the two phases. The corresponding SINR can be represented as:

$$\gamma_d^{\text{MRC}}[n] = \gamma_d^{(1)}[n] + \gamma_d^{(2)}[n], \forall n. \tag{17}$$

C. Problem Formulation

We first define the network's EE as the ratio of the sum rate to the total network's power consumption. That is $\eta_{EE}[n] =$

$\frac{R_{\text{sum}}[n]}{P_{\text{sum}}[n]}$, where $R_{\text{sum}}[n] = \log_2(1+\gamma_r^1[n]) + \log_2(1+\gamma_d^{\text{MRC}}[n])$. The total power consumption of the system can be considered as $P_{\text{sum}}[n] = \alpha_1[n] + \alpha_2[n] + P_c - P_t[n]$ where P_c represents the constant power consumption at the source. To maximize EE by optimizing the NOMA power allocation coefficients, PS ratio, and UAV trajectory, we formulate the following problem:

$$\text{P}_1: \max_{\rho[n],\alpha_1[n],\alpha_2[n],\boldsymbol{q}[n]} \sum\nolimits_{n=1}^{N} \eta_{EE}[n] \tag{18}$$

$$s.t.: \ \frac{1}{N}\sum\nolimits_{n=1}^{N} P_t[n] \geq \frac{1}{N}\sum\nolimits_{n=1}^{N} P[n], \tag{18a}$$

$$\gamma_{d\leftarrow r}^{(1)}[n] \geq \gamma_{\min}[n], \ \forall n, \tag{18b}$$

$$\gamma_d^{\text{MRC}}[n] \geq \gamma_{\min}[n], \ \forall n, \tag{18c}$$

$$0 < \rho[n] < 1, \ \forall n, \tag{18d}$$

$$P[n] \geq 0, \ \forall n, \tag{18e}$$

$$(1a) - (1c), (5a), (5b).$$

Constraint (18a) ensures the power harvested at the UAV for all time slots should be bigger than a minimum harvested power (we can safely assume this to be $P[n] = P_{\text{EH}}$). (18b) confirms the successful decoding of the destination node's data at the UAV, while (18c) ensures the minimum required SINR for the destination node. The PS-SWIPT ratio and the feasibility of the UAV's transmitted power are restrained by constraints (18d) and (18e), respectively.

III. A Two-Stage Solution to EE Problem

The problem (P_1) is non-convex NP-hard due to coupling among the optimization variables. Moreover, the objective function of (P_1) is in the form of sum-of-ratios, which is incompatible with conventional Dinkelbach method solutions [12], [13]. We propose a two-stage low-complexity algorithm, allowing for independent optimization of each variable.

A. Stage-one: Optimizing PS ratio and UAV trajectory

In this stage, the PS ratio and UAV's trajectory are designed iteratively with fixed NOMA power allocation coefficients. However, the sum rate function is non-convex due to the coupling between the PS ratio and UAV's trajectory variables. Hence, we solve the optimization problem in an iterative manner. Nonetheless, the non-linear fractional objective function first needs to be transformed into a subtractive form by utilizing the following theorem from [14].

Theorem [14]: Let suppose that $\rho^*[n]$ and $\boldsymbol{q}^*[n]$ are the optimal solutions to the problem (P_1). Then, the following optimization problem can provide an optimal solution in the existence of two vectors, namely, $\boldsymbol{\lambda} = [\lambda_1^*, ..., \lambda_N^*]^T$ and $\boldsymbol{\psi} = [\psi_1^*, ..., \psi_N^*]^T$ as follows:

$$\max_{\rho[n],\boldsymbol{q}[n]} \sum\nolimits_{n=1}^{N} \lambda_n^* \big[R_{\text{sum}}[n] - \psi_n^*(P_{\text{sum}}[n])\big]. \tag{19}$$

Furthermore, $\rho^*[n]$ and $\boldsymbol{q}^*[n]$ meet these two following equations:

$$R_{\text{sum}}^*[n] - \psi_n^*(P_{\text{sum}}[n]) = 0, \forall n, \tag{20}$$

$$1 - \lambda_n^*(P_{\text{sum}}[n]) = 0, \forall n. \tag{21}$$

Specifically, the equivalent subtractive form in (19) with the additional parameters $\{\boldsymbol{\lambda}^*, \boldsymbol{\psi}^*\}$ has the same optimal solution as (P_1) for given $\alpha_1[n]$ and $\alpha_2[n]$. In particular, the problem (19) can be solved iteratively with a two-layer approach, i.e., inner and outer layers. In the inner layer, (19) is solved under given $\boldsymbol{\lambda}$ and $\boldsymbol{\psi}$. Then, the two equations (20) and (21) are updated in the outer layer to obtain $\{\boldsymbol{\lambda}^*, \boldsymbol{\psi}^*\}$.

*1) **Inner-layer Problem**:* The inner layer optimization problem is non-convex. Therefore, we first optimize the PS ratio while considering a predetermined UAV trajectory and fixed NOMA power coefficients. Thus, the optimization problem for the PS ratio can be formulated as follows:

$$\text{P}_2: \max_{\rho[n]} \sum\nolimits_{n=1}^{N} \lambda_n^* \big[R_{\text{sum}}[n] - \psi_n^*(P_{\text{sum}}[n])\big] \tag{22}$$

$$s.t.: \quad (18a) - (18e).$$

The problem (P_2) is a convex optimization problem with respect to $\rho[n]$ and can be solved efficiently. Subsequently, we optimize the trajectory under the optimal PS ratio as follows:

$$\text{P}_3: \max_{\boldsymbol{q}[n]} \sum\nolimits_{n=1}^{N} \lambda_n^* \big[R_{\text{sum}}[n] - \psi_n^*(P_{\text{sum}}[n])\big] \tag{23}$$

$$s.t.: \quad \sum\nolimits_{n=1}^{N} \frac{\eta\rho[n]\beta_0^2 e^{-\xi(\|\boldsymbol{q}[n]-\boldsymbol{s}[n]\|)}}{\|\boldsymbol{q}[n]-\boldsymbol{s}[n]\|^2} \geq \sum_{n=1}^{N} P[n], \tag{23a}$$

$$\frac{\alpha_2[n]}{\alpha_1[n]+x\|\boldsymbol{q}[n]-\mathbf{s}[n]\|^2 e^{\xi(\|\boldsymbol{q}[n]-\boldsymbol{s}[n]\|)}} \geq \gamma_{\min}[n], \ \forall n, \tag{23b}$$

$$\frac{\alpha_2[n]\ |h_{sd}[n]|^2}{\alpha_1[n]\ |h_{sd}[n]|^2+\delta_1^2[n]} + \frac{\eta\rho[n]\beta_0^4}{\delta_2^2[n]} \cdot \frac{e^{-\xi(\|\boldsymbol{q}[n]-\boldsymbol{s}[n]\|+\|\boldsymbol{q}[n]-\boldsymbol{d}[n]\|)}}{\|\boldsymbol{q}[n]-\boldsymbol{s}[n]\|^2\ \|\boldsymbol{q}[n]-\boldsymbol{d}[n]\|^2} \geq \gamma_{\min}[n], \ \forall n, \tag{23c}$$

$$(1a) - (1c), (18e),$$

where $x = \frac{N}{1-\rho[n]\beta_0^2}$. The problem ($\text{P}_3$) is still non-convex. Hence, we transform (P_3) into its equivalent form by introducing slack optimization variables as follows:

$$\text{P}_4: \max_{\boldsymbol{q}[n],v[n],t[n],a[n],b[n]} \sum\nolimits_{n=1}^{N} \lambda_n^* \big[R_{\text{sum}}[n] - \psi_n^*(P_{\text{sum}}[n])\big] \tag{24}$$

$$s.t.: \quad \sum\nolimits_{n=1}^{N} \frac{\eta\rho[n]\beta_0^2}{e^{a[n]}} \geq \sum\nolimits_{n=1}^{N} P[n], \tag{24a}$$

$$\frac{\alpha_2[n]}{\alpha_1[n]+xe^{a[n]}} \geq \gamma_{\min}[n], \ \forall n, \tag{24b}$$

$$\frac{\alpha_2[n]\ |h_{sd}[n]|^2}{\alpha_1[n]\ |h_{sd}[n]|^2+\delta_1^2[n]} + \frac{\eta\rho[n]\beta_0^4}{\delta_2^2[n]e^{a[n]+b[n]}} \geq \gamma_{\min}[n], \forall n, \tag{24c}$$

$$v[n] \leq \frac{\|\boldsymbol{q}[n]-\boldsymbol{s}[n]\|^2}{e^{-\xi\|\boldsymbol{q}[n]-\boldsymbol{s}[n]\|}}, \ t[n] \leq \frac{\|\boldsymbol{q}[n]-\boldsymbol{d}[n]\|^2}{e^{-\xi\|\boldsymbol{q}[n]-\boldsymbol{d}[n]\|}}, \forall n, \tag{24d}$$

$$v[n] \leq e^{a[n]}, \quad t[n] \leq e^{b[n]}, \forall n, \tag{25e}$$

$$(1a) - (1c), (18e),$$

where

$$R_{\text{sum}}[n] = \log_2\left(1 + \left(\frac{(1-\rho[n])\alpha_1[n]\beta_0^2}{N} \cdot \frac{1}{e^{a[n]}}\right)\right) + \log_2\left(1 + \gamma_d^{(1)}[n] + \left(\frac{\eta\rho[n]\beta_0^4}{\delta_2^2[n]} \cdot \frac{1}{e^{a[n]+b[n]}}\right)\right). \tag{25}$$

Using the above transformations, the objective function and constraints are now convex functions, albeit intractable. Consequently, we exploit successive convex approximation (SCA)-based first-order Taylor expansions to approximate the problem (P_4) by convex ones iteratively. The first-order lower bounds are given by:

$$e^{a[n]} \geq e^{a^{(k)}[n]}(1 + a[n] - a^{(k)}[n]) \triangleq \tilde{e}^{a[n]}, \forall n, \tag{26}$$

$$e^{b[n]} \geq e^{b^{(k)}[n]}(1 + \ b[n] - b^{(k)}[n]) \triangleq \tilde{e}^{b[n]}, \forall n, \tag{27}$$

$$\frac{\|\boldsymbol{q}[n]-\boldsymbol{s}[n]\|^2}{e^{-\xi\|\boldsymbol{q}[n]-\boldsymbol{s}[n]\|}} \geq \frac{\left\|\boldsymbol{q}^{(k)}[n]-\boldsymbol{s}[n]\right\|^2}{e^{-\xi\left\|\boldsymbol{q}^{(k)}[n]-\boldsymbol{s}[n]\right\|}}+(2+\xi\|\boldsymbol{q}^{(k)}[n]-\boldsymbol{s}[n]\|)\cdot \frac{(\boldsymbol{q}^{(k)}[n]-\boldsymbol{s}[n])^T(\boldsymbol{q}[n]-\boldsymbol{q}^{(k)}[n])}{e^{-\xi\left\|\boldsymbol{q}^{(k)}[n]-\boldsymbol{s}[n]\right\|}} \triangleq \frac{\|\tilde{\boldsymbol{q}}[n]-\boldsymbol{s}[n]\|^2}{e^{-\xi\|\tilde{\boldsymbol{q}}[n]-\boldsymbol{s}[n]\|}}, \forall n, \quad (28)$$

$$\frac{\|\boldsymbol{q}[n]-\boldsymbol{d}[n]\|^2}{e^{-\xi\|\boldsymbol{q}[n]-\boldsymbol{d}[n]\|^2}} \geq \frac{\left\|\boldsymbol{q}^{(k)}[n]-\boldsymbol{d}[n]\right\|^2}{e^{-\xi\left\|\boldsymbol{q}^{(k)}[n]-\boldsymbol{d}[n]\right\|}}+(2+\xi\|\boldsymbol{q}^{(k)}[n]-\boldsymbol{d}[n]\|)\cdot \frac{(\boldsymbol{q}^{(k)}[n]-\boldsymbol{d}[n])^T(\boldsymbol{q}[n]-\boldsymbol{q}^{(k)}[n])}{e^{-\xi\left\|\boldsymbol{q}^{(k)}[n]-\boldsymbol{d}[n]\right\|}} \triangleq \frac{\|\tilde{\boldsymbol{q}}[n]-\boldsymbol{d}[n]\|^2}{e^{-\xi\|\tilde{\boldsymbol{q}}[n]-\boldsymbol{d}[n]\|^2}}, \forall n, \quad (29)$$

where $e^{a^{(k)}[n]}$ and $e^{b^{(k)}[n]}$ express the Taylor points at iteration k. According to the above transformation, the problem (P_4) can be approximated as:

$$\mathrm{P}_5: \max_{\boldsymbol{q}[n],v[n],t[n],a[n],b[n]} \sum\nolimits_{n=1}^{N} \lambda_n^*\left[\tilde{R}_{\text{sum}}[n]-\psi_n^*(P_{\text{sum}}[n])\right] \quad (30)$$

$$s.t.: \quad \sum\nolimits_{n=1}^{N} \frac{\eta\rho[n]\beta_0^2}{\tilde{e}^{a[n]}} \geq \sum\nolimits_{n=1}^{N} P[n], \quad (30a)$$

$$\frac{\alpha_2[n]}{\alpha_1[n]+x\tilde{e}^{a[n]}} \geq \gamma_{\min}[n], \ \forall n \quad (30b)$$

$$\frac{\alpha_2[n]\ |h_{sd}[n]|^2}{\alpha_1[n]|h_{sd}[n]|^2+\delta_1^2[n]}+\frac{\eta\rho[n]\beta_0^4}{\delta_2^2[n]\tilde{e}^{a[n]+b[n]}} \geq \gamma_{\min}[n], \forall n, \quad (30c)$$

$$v[n] \leq \frac{\|\tilde{\boldsymbol{q}}[n]-\boldsymbol{s}[n]\|^2}{e^{-\xi\|\tilde{\boldsymbol{q}}[n]-\boldsymbol{s}[n]\|}}, t[n] \leq \frac{\|\tilde{\boldsymbol{q}}[n]-\boldsymbol{d}[n]\|^2}{e^{-\xi\|\tilde{\boldsymbol{q}}[n]-\boldsymbol{d}[n]\|}}, \forall n, \quad (30d)$$

$$v[n] \leq \tilde{e}^{a[n]}, \quad t[n] \leq \tilde{e}^{b[n]}, \forall n, \quad (30e)$$

$$(1a)-(1c), (18e),$$

where $\tilde{R}_{\text{sum}}[n] = R_{\text{sum}}[n]|_{e^{a}[n]=\tilde{e}^{a[n]}, e^{b}[n]=\tilde{e}^{b[n]}}$. The problem ($\mathrm{P}_5$) can be solved at iteration k by employing convex optimization solvers, e.g., CVX [13].

*2) **Outer-layer Problem**:* In this layer, an iterative algorithm based on the damped Newton method is utilized to find $\{\boldsymbol{\lambda}, \boldsymbol{\psi}\}$. Let us define $\phi_n(\psi_n) = R_{\text{sum}}^*[n] - \psi_n^*(P_{\text{sum}}[n])$ and $\phi_{N+j}(\lambda_j) = 1 - \lambda_j^*(P_{\text{sum}}[j])$, $j \in \{1, ..., N\}$. It is demonstrated in [2] that the optimal solution $\{\boldsymbol{\lambda}^*, \boldsymbol{\psi}^*\}$ is found if and only if $\phi(\boldsymbol{\lambda}, \boldsymbol{\psi}) = [\phi_1, \phi_2, ..., \phi_{2N}]^T = 0$. Accordingly, the updated value of the $\boldsymbol{\lambda}^{i+1}$ and $\boldsymbol{\psi}^{i+1}$ in the iteration i can be obtained by:

$$\boldsymbol{\lambda}^{i+1} = \boldsymbol{\lambda}^i + \zeta^i \boldsymbol{v}_{N+1:2N}^i, \quad (31)$$

$$\boldsymbol{\psi}^{i+1} = \boldsymbol{\psi}^i + \zeta^i \boldsymbol{v}_{1:N}^i, \quad (32)$$

where $\boldsymbol{v} = [\acute{\phi}(\boldsymbol{\lambda}, \boldsymbol{\psi})]^{-1}\phi(\boldsymbol{\lambda}, \boldsymbol{\psi})$, and $\acute{\phi}(\boldsymbol{\lambda}, \boldsymbol{\psi})$ is the Jacobian matrix of $\phi(\boldsymbol{\lambda}, \boldsymbol{\psi})$. Moreover, ζ^i is the largest value of Ξ^m satisfying

$$\|\phi(\boldsymbol{\lambda}^i+\Xi^m\boldsymbol{v}_{N+1:2N}^i, \boldsymbol{\psi}^i+\Xi^m\boldsymbol{v}_{1:N}^i)\| \leq (1-\varepsilon\Xi^m)\|\phi(\boldsymbol{\lambda}, \boldsymbol{\psi})\|, \quad (33)$$

where $m \in \{1, 2, ...\}$, $\Xi^m \in (0, 1)$, and $\varepsilon \in (0, 1)$.

B. Stage-two: Optimizing power coefficients

A new framework is proposed in this stage. Consider a sum-fraction problem formulated as follows:

$$\min_{\boldsymbol{\Omega}\in C} \sum_{j=1}^{J} \frac{B_j(\boldsymbol{\Omega})}{A_j(\boldsymbol{\Omega})}, \quad (34)$$

where J is the maximum number of fractional terms, and $\boldsymbol{\Omega}$ is the optimization variable vector with the domain of C. In the following, it is demonstrated that (34) has an equivalent form, which is:

$$\min_{\boldsymbol{\Omega}\in C, \iota_j>0} \sum_{j=1}^{J} \iota_j B_j^2(\boldsymbol{\Omega}) + \sum_{j=1}^{J} \frac{1}{4\iota_j}\frac{1}{A_j^2(\boldsymbol{\Omega})}. \quad (35)$$

In fact, the solution to both (34) and (35) is the same. It is noteworthy that if $A_j(\boldsymbol{\Omega})$ is a concave function and $B_j(\boldsymbol{\Omega})$ is a convex one, then the problem (35) is convex quadratic for the given ι_j. Based on the above analysis, the convex problem (35) is solved for a given $\iota_j = \frac{1}{2A_j(\boldsymbol{\Omega})B_j(\boldsymbol{\Omega})}$, and then the value of ι_j will be updated in the next iteration. Consequently, with a specified PS ratio and UAV trajectory, problem (P_1) can be represented in the following equivalent manner:

$$\mathrm{P}_6: \min_{\alpha_1[n],\alpha_2[n],\iota[n]>0} \sum_{n=1}^{N} \iota[n]P_{\text{sum}}^2[n] + \sum_{n=1}^{N} \frac{1}{4\iota[n]}\frac{1}{R_{\text{sum}}^2[n]} \quad (36)$$

$$s.t.: \quad \frac{\alpha_2[n]|h_{sr}[n]|^2}{\gamma_{\min}[n]} - \alpha_1[n]|h_{sr}[n]|^2 \geq \frac{N}{(1-\rho[n])}, \ \forall n, \quad (36a)$$

$$\alpha_2[n]|h_{sd}[n]|^2 - \alpha_1[n]|h_{sd}[n]|^2\chi \geq \delta_1^2[n]\chi, \ \forall n, \quad (36b)$$

$$(5a), (5b), (18e),$$

where $\chi = \gamma_{\min} - \frac{\eta\rho[n]|h_{sr}[n]|^2|h_{rd}[n]|^2}{\delta_2^2[n]}$, and $\iota[n] = \frac{1}{2P_{\text{sum}}^2[n]R_{\text{sum}}^2[n]}$. It can be observed that all constraints are linear and convex. Nevertheless, the objective function is non-convex due to the non-concavity of the sum rate function. To deal with this issue, we utilize the result of the following corollary [13].

Corollary 1: Consider $\mathcal{F}$ as a decreasing function, then

$$\min_{\boldsymbol{\Upsilon}\in C} \sum_{j=1}^{J} \mathcal{F}_j\left(\frac{\mathcal{A}_j(\boldsymbol{\Upsilon})}{\mathcal{B}_j(\boldsymbol{\Upsilon})}\right), \quad (37)$$

is equivalent to the following problem:

$$\min_{\boldsymbol{\Upsilon}\in C, \varrho_j} \sum_{j=1}^{J} \mathcal{F}_j(2\varrho_j\sqrt{\mathcal{A}_j(\boldsymbol{\Upsilon})} - \varrho_j^2\mathcal{B}_j(\boldsymbol{\Upsilon})), \quad (38)$$

with the updated value of $\varrho_j = \frac{\sqrt{\mathcal{A}_j(\boldsymbol{\Upsilon})}}{\mathcal{B}_j(\boldsymbol{\Upsilon})}$.

By adopting the result of Corollary 1, the second term of the objective function in (P_6) can be equivalently written as:

$$\min_{\alpha_1[n],\alpha_2[n],\varrho[n]} \sum_{n=1}^{N} \frac{1}{4\iota[n]}\frac{1}{\hat{R}_{\text{sum}}^2[n]} \quad (39)$$

where

$$\hat{R}_{\text{sum}}[n] = \log_2(1+\gamma_r^1[n]) + \log_2\Big(1+\gamma_d^2[n] + 2\varrho[n]\sqrt{\alpha_2[n]\ |h_{sd}[n]|^2} - \varrho^2[n](\alpha_1[n]\ |h_{sd}[n]|^2 + \delta_1^2[n])\Big), \quad (40)$$

where $\varrho[n] = \frac{\sqrt{\alpha_2[n]\ |h_{sd}[n]|^2}}{\alpha_1[n]\ |h_{sd}[n]|^2+\delta_1^2[n]}$. $\hat{R}_{\text{sum}}[n]$ is now biconcave with respect to the power allocation coefficients and $\varrho[n]$. Accordingly, the multi-convex optimization problem can be formulated as:

$$\mathrm{P}_7: \min_{\boldsymbol{\alpha}[n],\varrho[n]} \sum_{n=1}^{N} \iota[n]P_{\text{sum}}^2[n] + \sum_{n=1}^{N} \frac{1}{4\iota[n]}\frac{1}{\hat{R}_{\text{sum}}^2[n]} \quad (42)$$

$$s.t.: \quad (5a), (5b), (18e), (36a), (36b),$$

where $\boldsymbol{\alpha}[n] = [\alpha_1[n], \alpha_2[n]] \in \mathbb{R}^{2\times 1}$. We note that $P_{\text{sum}}[n]$ is a function of power allocation coefficients, and every coefficient has its own constraint. Hence, the terms of $P_{\text{sum}}[n]$ and $\hat{R}_{\text{sum}}[n]$ are decoupled to optimize $P_{\text{sum}}[n]$ distributively. The problem (P_7) is now convex and can be solved [13].

IV. Simulation Results and Discussions

For our simulation, we consider a square region with dimensions of 30 m × 30 m, which accommodates one user

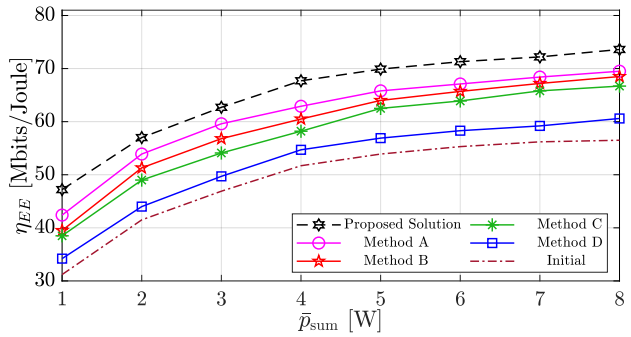

Fig. 2. EE users vs. $\bar{p}_{\text{sum}}$

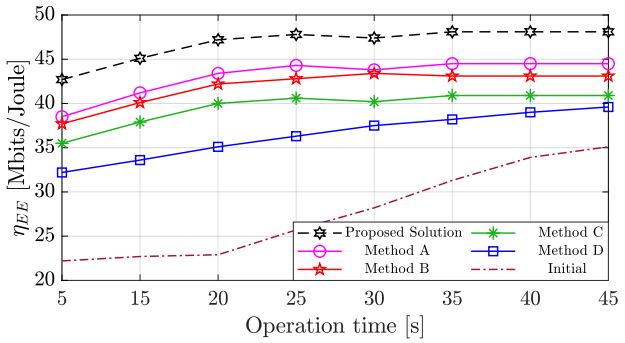

Fig. 3. EE users vs. operation time

and a single UAV, both positioned randomly. To avoid peaks in path loss, we set the carrier frequency at $f = 1.2$ THz and the transmission bandwidth at 10 GHz. Considering water vapor's significant influence on molecular absorption loss, we relate the frequency-dependent absorption coefficient $\xi(f)$ solely to water vapor molecules [10]. Additional parameters adhere to the ones specified in [5], [10] and the references within.

Fig. 2 presents the EE performance as a function of the average network transmission power parameter, $\bar{p}_{\text{sum}} = P_{\max} + P_{\text{peak}} + P_c - P_{\text{EH}}$. The curve marked as 'Initial' represents the EE performance with a non-optimal feasible (random) initialization of the UAV trajectory. Importantly, our proposed algorithm consistently demonstrates higher performance gaps than other benchmark designs, with the relative gap slightly widening as $\bar{p}_{\text{sum}}$ increases. For comparison, Fig. 2 also investigates the average EE of four methods. Method A investigates the proposed algorithm based on the NOMA scheme, where the NOMA power coefficient is considered fixed. Method B analyzes the performance superiority between our system's two access schemes, NOMA and OMA. Method C examines our proposed algorithm with a pre-defined UAV trajectory, while Method D considers the scenario with constant ($\rho[n] = 0.5, \forall n$) PS factors. Our proposed algorithm outperforms these benchmarks by $30.3\%, 23.0\%, 21.2\%$, and $18.1\%, 7.26\%$, respectively, compared to the case with no trajectory optimization.

Fig. 3 examines the influence of mission time (T) on EE performance across various schemes. It is evident that EE rises as T progresses for the fixed trajectory schemes (Method D) and the non-optimal initial feasible scheme (Initial). However, this uniform increase is less visible in the other schemes (Methods A, B, and C). Increased mission time can boost EE performance by at least respectively $37.1\%, 26.8\%, 22.8\%$, and $16.5\%, 12.8\%$ with regard to initial UAV trajectory deployment, as it allows for extended periods of communication and flight parameter adjustments. Moreover, the interplay between optimization variables leads to a non-monotonic EE growth, yet an overall increasing trend in EE performance as T grows. It is also worth noting that minimizing the task completion time of the considered UAV relay system for specific EE requirements is an exciting challenge that merits further investigation.

V. Conclusion

In this paper, we have presented a new strategy for deploying a UAV to facilitate wireless THz connectivity, explicitly accounting for the molecular absorption effect in the THz-enabled UAV path loss channel gain model. We have then formulated an optimization problem to maximize EE in NOMA-SWIPT cooperative UAV network while satisfying quality of service requirements. To tackle this problem, we have introduced an iterative algorithm that partitions the original optimization problem into three tractable subproblems based on a two-stage approach. These focus on optimizing the decision variables: the UAV's location, PS-SWIPT ratio, and the NOMA power allocation coefficients. Our simulation results indicate that the proposed algorithm significantly boosts the network's EE performance compared to baseline algorithms.

References

[1] M. Mozaffari, W. Saad, M. Bennis, Y.-H. Nam, and M. Debbah, "A tutorial on UAVs for wireless networks: Applications, challenges, and open problems," *IEEE Commun. Surv. Tutor.*, vol. 21, pp. 2334–2360, Q3 2019.

[2] J. Jalali, A. Khalili, A. Rezaei, J. Famaey, and W. Saad, "Power-efficient antenna switching and beamforming design for multi-user SWIPTwith non-linear energy harvesting," in *2023 IEEE 20th Consumer Commun. Netw. Conf*, pp. 746–751, 2023.

[3] H. Peng and L.-C. Wang, "Energy harvesting reconfigurable intelligent surface for UAV based on robust deep reinforcement learning," *IEEE Trans. Wirel. Commun.*, pp. 1–1, 2023.

[4] M. Hua, C. Li, Y. Huang, and L. Yang, "Throughput maximization for UAV-enabled wireless power transfer in relaying system," in *2017 9th Int. Conf. Wirel. Commun. Signal Proc.*, pp. 1–5, 2017.

[5] S. Yin, Y. Zhao, L. Li, and F. R. Yu, "UAV-assisted cooperative communications with power-splitting information and power transfer," *IEEE Trans. Green Commun. Netw*, vol. 3, pp. 1044–1057, Dec. 2019.

[6] X. Sun, W. Yang, and Y. Cai, "Secure communication in NOMA-assisted millimeter-wave SWIPT UAV networks," *IEEE Internet Things J.*, vol. 7, no. 3, pp. 1884–1897, 2020.

[7] C. Chaccour, M. N. Soorki, W. Saad, M. Bennis, P. Popovski, and M. Debbah, "Seven defining features of terahertz (THz) wireless systems: A fellowship of communication and sensing," *IEEE Commun. Surv. Tutor.*, vol. 24, pp. 967–993, Q2 2022.

[8] S. B. Melhem and H. Tabassum, "User pairing and outage analysis in multi-carrier noma-thz networks," *IEEE Transactions on Vehicular Technology*, vol. 71, no. 5, pp. 5546–5551, 2022.

[9] L. Xu, M. Chen, M. Chen, Z. Yang, C. Chaccour, W. Saad, and C. S. Hong, "Joint location, bandwidth and power optimization for THz-enabled UAV communications," *IEEE Commun. Lett.*, vol. 25, pp. 1984–1988, Jun. 2021.

[10] Q. Li, A. Nayak, Y. Zhang, and F. R. Yu, "A cooperative recharging-transmission strategy in powered UAV-aided terahertz downlink networks," *IEEE Trans. Veh. Technol.*, vol. 72, pp. 5479–5484, Apr. 2023.

[11] N. Iradukunda, Q.-V. Pham, Z. Ding, and W.-J. Hwang, "THz-enabled UAV communications using non-orthogonal multiple access," *IEEE Trans. Veh. Technol.*, pp. 1–6, 2023.

[12] W. Dinkelbach, "On nonlinear fractional programming," *J. Manag. Sci.*, vol. 13, no. 3, p. 492–498, 1967.

[13] J. Jalali, A. Khalili, A. Rezaei, R. Berkvens, M. Weyn, and J. Famaey, "IRS-based energy efficiency and admission control maximization for IoT users with short packet lengths," *IEEE Trans. Veh. Technol.*, pp. 1–6, 2023.

[14] Y. Jong, *An efficient global optimization algorithm for nonlinear sum-of-ratios problem*. Center of Natural Science, University of Sciences, Pyongyang, DPR Korea, May 2012.